DOI: 10.1002/ecs2.4101

ARTICLE

Methods, Tools, and Technologies



Uncertainty in parameterizing a flux-based model of vegetation carbon phenology using ecosystem respiration

Yuan Gong^{1,2,3} | Christina L. Staudhammer² | Susanne Wiesner^{2,4} | Jeffery B. Cannon⁵ | Gregory Starr² | Yinlong Zhang¹

Correspondence

Yinlong Zhang Email: zylnjfu@gmail.com

Funding information

Priority Academic Program Development of Jiangsu Higher Education Institutions; National Key Research and Development Program of China, Grant/Award Number: 2016YFC0502704; US National Science Foundation, Grant/Award Numbers: DEB EF-1241881, DEB EF-1702029

Handling Editor: Theresa M. Crimmins

Abstract

The seasonal dynamics of plant communities are important indicators for assessment of long-term vegetation patterns and provide valuable information to predict ecosystem responses to climate change. However, increased frequency of extreme weather events can force ecosystems into unstable states, which leads to greater uncertainty in determining phenological metrics (e.g., growing season length). To better understand these uncertainties, we utilized 9 years of eddy covariance and remote sensing data to parameterize models of seasonal ecosystem respiration (Re) for two subtropical longleaf pine forests (mesic and xeric), with similar vegetation but different water holding capacity. We compared two commonly used algorithms to extract phenology metrics, the growth rate (GR) and third derivative (TD) methods, which are usually used without justification. We determined the impact of algorithm selection on estimating key biological dates related to plant community carbon dynamics (e.g., start, end, and length of physiologically active season, specifically Re), characterized the model's response to extreme weather events, and compared estimates to those derived via remotely sensed greenness from the enhanced vegetation index (EVI). We observed that periods of winter warming increased duration of physiological activity in terms of Re, and summer water limitation caused multi-peaked, asymmetric behavior, creating significant uncertainties. We found that choice of phenology metric extraction algorithm significantly impacted biological event dates; the GR method estimated longer phenophases than the TD in both sites, as well as earlier starting and later ending dates for phenophases. Because the TD method was unable to give estimates during the buffer period of phenophase transition under certain weather conditions, the GR method may be more suitable for studies in subtropical forests. Dates derived from EVI greenness rarely matched those of plant community seasonal dynamics models, especially in spring and summer. The estimated length of Re from the model was significantly longer than that derived from EVI, indicating that the use of EVI could result in shorter growing season estimates and

This is an open access article under the terms of the Creative Commons Attribution License, which permits use, distribution and reproduction in any medium, provided the original work is properly cited.

¹Co-Innovation Center for Sustainable Forestry in Southern China, College of Biology and the Environment, Nanjing Forestry University, Nanjing, China

²Department of Biological Sciences, The University of Alabama, Tuscaloosa, Alabama, USA

³Department of Geographic Information Science, School of Geographic Information and Tourism, Chuzhou University, Chuzhou, China

⁴Department of Biological Systems Engineering, University of Wisconsin-Madison, Madison, Wisconsin, USA

⁵The Jones Center at Ichauway, Newton, Georgia, USA

^{© 2022} The Authors. Ecosphere published by Wiley Periodicals LLC on behalf of The Ecological Society of America.

greater uncertainty. Our results provide direction for optimization of future approaches to extract phenological metrics and better scientific understanding of forest land surface phenology, as weather anomalies become more common with climate change.

KEYWORDS

ecosystem phenology, eddy covariance, enhanced vegetation index, growth rate, logistic function, longleaf pine forest, third derivative

INTRODUCTION

Forests play an important role in global carbon cycles (García-Oliva & Jaramillo, 2011; Gong et al., 2019; Wiesner et al., 2020). Their physiological response to global climate change has long been an area of research focus, as forests provide ecosystem services to offset climate change (Aber et al., 2001; Griscom et al., 2017). Forest physiology is sensitive to climate change, responding to alterations in temperature, precipitation, atmospheric CO₂ concentrations, and modifications in the frequency and intensity of disturbance and extreme events (Kirilenko & Sedjo, 2007). A better understanding of the variability of the physiological functions of forests at different temporal and spatial scales is of great value in quantifying responses to climate change (Aber et al., 2001; Berra & Gaulton, 2021; Gong et al., 2020).

Observing carbon dioxide (CO₂) fluxes is one of the main methods used to quantify ecosystem physiological activity and key phenological metrics (Baldocchi, 2003, 2008; Gong & Zhang, 2020; Wu & Chen, 2013). Net ecosystem productivity (NEP) and gross primary productivity (GPP) derived from eddy covariance (EC) observations have been widely utilized to understand system responses to climate variation, disturbance regimes, and management practices in different ecosystems across the globe (Gonsamo et al., 2015; Wiesner et al., 2021). Recent studies have also utilized EC data with phenological approaches (i.e., curve reconstruction and extraction of phenological metrics; Kross et al., 2014) to understand key phenology communities indicators across plant (Gonsamo et al., 2015). Phenology metrics can then be estimated, including the length of the growing season, to describe vegetation carbon phenology (VCP; i.e., the start and end points of a specific phenophase; Kong et al., 2020). Key metrics of VCP for an ecosystem can be extracted through fixed threshold, growth rate, or third derivative (TD) approaches, ultimately quantifying the response of physiological functions to seasonal cues and climatic variables (Gonsamo et al., 2013; Gu et al., 2009; Jin et al., 2017).

In addition to climatic drivers, vegetation greenness has been reported to be a driver of VCP (Kong et al., 2020; Wu

et al., 2014). Vegetation greenness can easily be determined with remotely sensed data, such as the enhanced vegetation index (EVI); however, data derived from EC methods may be more useful for building a mechanistic understanding of phenology. Relative agreement between EC observations and remote sensing products can also provide reference for the optimization of phenological algorithms. Models of plant community seasonal dynamics and their associated estimated metrics of ecosystem productivity (i.e., peak day and stable period) are powerful tools to advance our understanding of changes in the functions of forests (Gong et al., 2020; Gu et al., 2009; Niu et al., 2013).

Consistent with ecosystem productivity, ecosystem respiration (Re) is an essential measurement used to understand forest physiology (Noormets et al., 2009; Starr et al., 2015, 2016). Most of the current VCP research focuses on GPP or NEP, while VCP metrics derived from Re are still nascent. While patterns of Re are often described as the difference between GPP and NEP (Starr et al., 2015), mathematically characterizing Re derived from plant community seasonal dynamics models (i.e., Re-derived VCP) could advance knowledge of forest function (Yang & Noormets, 2020). For example, Kross et al. (2014) fit models to extract dates of the maximum and minimum values in the rate of change (first derivative) of Re, while Liu et al. (2021) extracted the dates of the start, end, and peak day of modeled Re with a fixed threshold method. Recently, Yang and Noormets (2020) utilized logistic functions to model ecosystem Re and extract complete phenological metrics (flux development rate, transition date, and phenological duration). However, there is a lack of climatic and biological explanations of the phenological characteristics associated with Re for different ecosystems (Liu et al., 2021).

Like GPP-derived VCP, Re-derived VCP is affected by environmental factors (e.g., temperature and precipitation patterns) and strongly correlated with spectral-based vegetation greenness (Kong et al., 2020; Noormets et al., 2009; Yuste et al., 2003). These factors control the dates of key biological events related to VCP, such as phenophases and vegetation growth (Kross et al., 2014). Re-derived VCP event dates are estimated to give quantities such as the

ECOSPHERE 3 of 17

start of respiration (SOR), the end of respiration (EOR), and the length of respiration season (LOR; days between SOR and EOR) (Noormets et al., 2009; Wu & Chen, 2013). Estimates of these phenological dates are usually derived assuming the behavior of the response variable (e.g., GPP, Re, or vegetation index) is symmetrical and unimodal (Luo et al., 2019; Younes et al., 2020; Zhou, 2018). However, due to various local and/or regional weather anomalies, forests may enter an unstable state (Wiesner et al., 2021), which can cause fluctuations in forest VCP (Starr et al., 2016; Yang & Noormets, 2020). This introduces a significant amount of variability in an ecosystem's response, which makes it challenging to determine reasonable phenology metrics (Yang & Noormets, 2020). Furthermore, Re is an important medium for decomposing GPP from NEP and highly sensitive to temperature variation (Jones et al., 2003). A better understanding of Re-derived VCP can improve our ability to quantify ecosystem responses to climate change.

Re can also be used to parameterize plant community models to better quantify biological and nonbiological disturbances in these systems (Yang & Noormets, 2020). While simple functions may not be able to describe shortterm variation in ecosystem VCP (J. Wang et al., 2018; Yang & Noormets, 2020), the nine-parameter function developed by Gu et al. (2009) has been shown to have flexibility in describing vegetation phenology responses (Gong et al., 2019, 2021). The model also has better performance when describing ecosystem VCP under abnormal environmental conditions (Yang & Noormets, 2020). In addition to choosing a suitable functional form, this type of phenological approach requires the selection of a biologically reasonable algorithm to extract VCP metrics (Wu et al., 2017; Zhou, 2018). For example, with the growth rate approach (Gu et al., 2009), VCP metrics (e.g., SOR and EOR) are assigned based on the locations of extreme values in the daily change of modeled Re. The TD approach (Gonsamo et al., 2013), in contrast, finds VCP metrics using extrema of the TD of Re. While the choice of algorithm is invariably made without discussion, different VCP metrics may result from them in some locations. Zhou (2018) found differences in these metrics derived from PhenoCam data when comparing four methods in three US forest sites. Because seasonal variation is slower in the subtropical zone, there is a longer phenological transition with weak growing season amplitude, compared temperate and continental regions et al., 2020). Thus, the GR method, which uses a dynamic threshold based on the maximum recovery rate, may indicate a longer LOR. However, there have been relatively few applications of plant community seasonal dynamics models using subtropical forest Re to parameterize them (Liu et al., 2021; Noormets et al., 2009; Yang & Noormets, 2020). Thus, there is a lack of comparative

research on the advantages and disadvantages of algorithm selection for forest VCP (Gong et al., 2020), which establishes the foundation for this study.

The goal of this study was to provide a new perspective for the application of plant community seasonal dynamics models for Re of subtropical forests, improve the current understanding of physiological functions of subtropical forest, and provide a technical reference and theoretical support for future research in other forests. We used EC measurements, meteorological, and satellite-based remote sensing greenness data over a nine-year period (2009–2017) from two subtropical evergreen coniferous forests. We applied the nine-parameter function developed by Gu et al. (2009), then examined the difference in derived VCP metrics from the TD and GR approaches. The goal of this research was to address the following hypotheses: (1) Phenological dates derived from vegetation greenness will be significantly correlated with Re-derived VCP metrics; (2) due to the higher air temperature in the subtropical region, the GR method—which is impacted by the steepness of the Re curve-will overestimate the LOR; and (3) summer water availability will cause instability in the inflection timing of Re in the peak phenophase, and the TD method will underestimate the length of peak period of Re. By testing these three hypotheses, we evaluate the differences, advantages, and disadvantages of the two algorithms to better understand the relationship between Re-derived VCP and vegetation greenness phenology. Similarities among results from these approaches will indicate under which conditions these models are robust, while divergence among results will indicate a need for further investigation.

MATERIALS AND METHODS

Study sites

Our study was conducted with data from two sites located at the Jones Center at Ichauway, a ~11,000-ha longleaf pine reserve in southwestern Georgia, USA (31.22° N, 84.47° W; Figure 1). The regional climate is subtropical (Wiesner et al., 2018). The long-term average annual precipitation of the area is 1310 mm, with most of the rainfall occurring from June to August. The longterm average annual air temperature is 19.1°C, with the lowest monthly average air temperature in January (10.7°C) and the highest monthly average temperature in June (27.4°C, Starr et al., 2015). While long-term winter (November to December) air temperature over the past 60 years has been estimated to be 13°C (Gong et al., 2021), an abnormal winter air temperature increase occurred during 2015 and 2016, with winter temperatures, which were \sim 3.8 and \sim 2.2°C higher than the long-

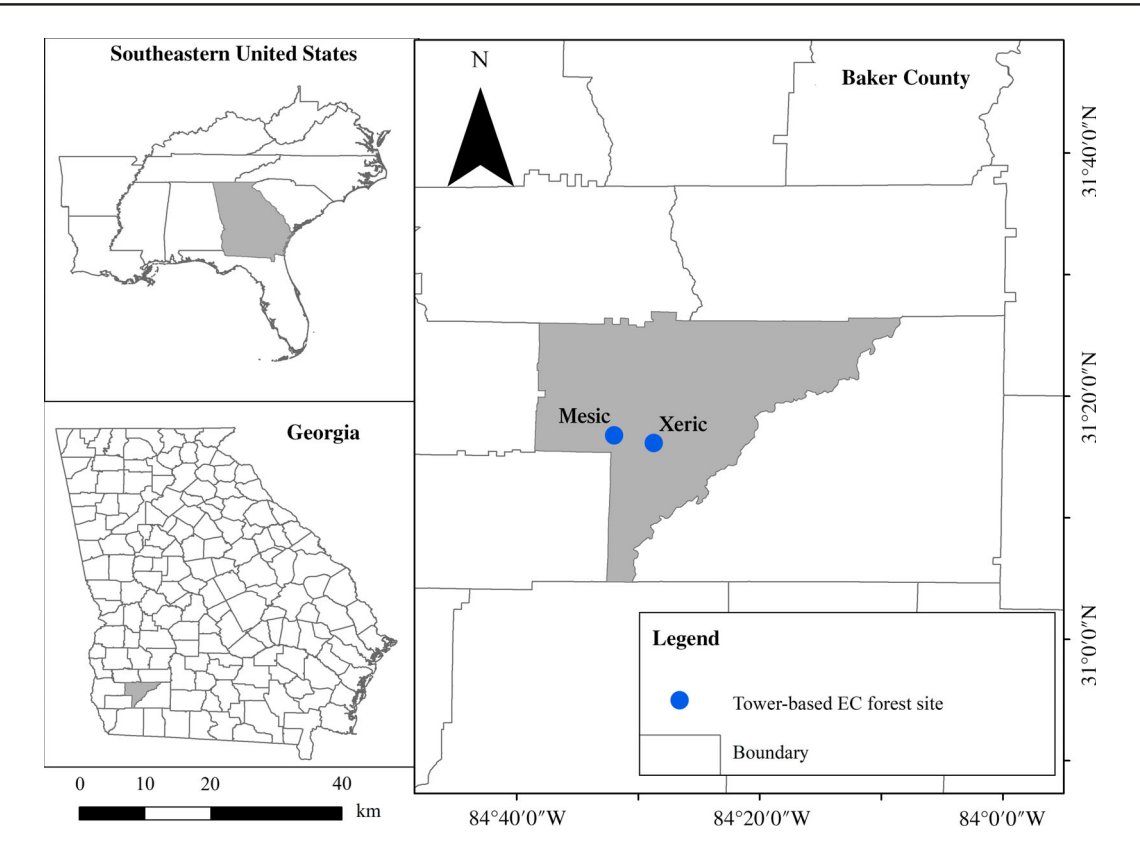


FIGURE 1 Geographical locations of two tower-based subtropical forest eddy covariance sites inside the Jones Center at Ichauway, USA. EC, eddy covariance

term average at both sites. The two sites are situated within 5 km of each other and differ in soil water holding capacity and forest structure (Table 1; Wiesner et al., 2020, 2021). The mesic site is at 65 m above sea level and lies on somewhat poorly drained sandy loam over sandy clay loam and clay-textured soils (Goebel et al., 1997). The xeric site is at 60 m above sea level and lies on well-drained deep sandy soils with no argillic horizon (Goebel et al., 1997). In the flux footprint area of the two EC towers, longleaf pine trees (Pinus palustris Mill.) are the dominant woody plants, averaging 100 years in age, and understory vegetation includes species such as Diospyros virginiana L. and Aristida stricta Michx (Kirkman et al., 2013; Wiesner et al., 2018). Low-intensity prescribed burns have been applied every 2 years during odd-numbered years (Wiesner et al., 2020, 2021). These burns have been shown to impact CO2 dynamics for \sim 30–60 days postfire (Whelan et al., 2013).

Net ecosystem CO₂ exchange measurements with EC approach

Net ecosystem CO₂ exchange (NEE; µmol CO₂ m⁻² s⁻¹) was estimated at the sites via open-path EC methods (Starr et al., 2015, 2016) using LI-COR CO₂/H₂O infrared gas analyzers (Li-7500, LI-COR, Lincoln, NE)

TABLE 1 Stand characteristics and mean environmental variables (± 1 SD) for the mesic and xeric longleaf pine study sites at the Jones Center at Ichauway in Georgia, USA

| at the solies center at lendaway | iii Georgia, Obri | |
|--|---------------------|---------------------|
| Stand characteristic | Mesic | Xeric |
| $B_{\rm A}$ all tree spp. (m ² ha ⁻¹) | $18.4~(\pm 1.7)$ | $11.1~(\pm 2.9)$ |
| $B_{\rm A}$ Pinus palustris (m 2 ha $^{-1}$) | $17.4 (\pm 2.1)$ | 8.2 (±3.8) |
| dbh (cm) | 25.7 (±15.2) | $18.1~(\pm 13.8)$ |
| Proportion of oak trees (%) | 8.0 | 22.0 |
| Wiregrass abundance (%) | 28 | 24 |
| Woody plant abundance (%) | 12 | 10 |
| Water holding capacity (cm m ⁻¹ ; upper 3 m soil) | 40 | 18 |
| EVI—growing season | $0.418~(\pm 0.046)$ | $0.412~(\pm 0.049)$ |
| EVI—nongrowing season | $0.314~(\pm 0.03)$ | $0.284~(\pm 0.03)$ |

Note: Growing season is defined as spring–summer, inclusive. Abbreviations: B_A , basal area; EVI, enhanced vegetation index; dbh, diameter at breast height.

accompanied by three-dimensional ultrasonic anemometers (CSAT-3, Campbell Scientific Instruments, Logan, UT). Each EC measurement system was installed approximately 4 m above mean canopy height (Starr et al., 2015, 2016). Tower heights were 34.4 and 34.9 m above ground, for the mesic and xeric sites, respectively, resulting in

ECOSPHERE 5 of 17

upwind flux source areas that extend a radius of approximately 500 m from each tower (Starr et al., 2015). Meteorological data, including photosynthetically active radiation (PAR; LI-190, LI-COR Inc.), global radiation (LI-200SZ, LI-COR Inc.), incident and outgoing shortwave and longwave radiation to calculate net radiation (NR01, Hukseflux Thermal Sensors, Delft, The Netherlands), precipitation (TE525 Tipping Bucket Rain Gauge, Texas Electronics, Dallas, TX), and air temperature and relative humidity (HMP45C, Campbell Scientific Instruments), were collected above the canopy and stored on CR-5000 dataloggers (Campbell Scientific Instruments).

Ecosystem respiration partitioning from EC-measured NEE

Flux data were processed with the EdiRe software (v.1.4.3.1184) at 30-min intervals, using a coordinate rotation, frequency response correction, WPL (Webb, Pearman, and Leuning; Webb et al, 1980) density correction, and spectral attenuation (Starr et al., 2015, 2016). QA/QC of the CO_2 flux data was maintained using stationarity criteria and integral turbulent statistics (Starr et al., 2015), and by filtering out data that did not pass plausibility tests (i.e., NEE < -30 and NEE > $30 \mu mol CO_2 m^{-2} s^{-1}$).

Missing and disqualified half-hourly CO2 flux data were gap-filled using separate functions for NEE during davtime nighttime. When and **PAR** was >10 µmol m⁻² s⁻¹, daytime NEE data were gap-filled using a Michaelis-Menten approach, and when PAR was <10 μmol m⁻² s⁻¹, nighttime NEE data were gap-filled using a modification of the Lloyd and Taylor (1994) approach, both on a monthly basis (Whelan et al., 2013). When too few observations were available to produce stable and biologically reasonable parameter estimates, we used annual equations to gap-fill daytime and nighttime NEE data by site. Half hourly fluxes of NEE in μmol CO₂ m⁻² s⁻¹ were used to calculate GPP and Re (Starr et al., 2015). Error estimation from gap-filled values of NEE was performed via bootstrap methods following Whelan et al. (2013). Bootstrap procedures were performed monthly or annually, where appropriate. Briefly, for each dataset of size n, synthetic datasets were generated by randomly selecting n observations with replacement from the original data. We generated 1000 synthetic datasets for each estimated gap-filling model (day and night models) and constructed the distribution of each model parameter. These distributions were then checked to ensure that the model parameters derived from the original data were contained within a 95% confidence region. In all cases, parameter estimates from the original data were within the 95% bootstrap confidence regions (Appendix S1: Tables S1 and S2).

Curve fitting and phenological metric extraction algorithms for Re

This study used a nine-parameter function (Gu et al., 2003, 2009) to model the interannual behavior in Re at each site and assess the potential impact of algorithmic differences on ecosystem-scale VCP metrics (Gonsamo et al., 2013; Gu et al., 2009). The flux-based function was originally developed utilizing interannual daily maximum GPP (μ mol CO₂ m⁻² s⁻¹) obtained from 30-min observations to quantify the phenological characteristics of plant community photosynthetic capacity (Gu et al., 2003, 2009). Recent studies have shown that this function performs well when parameterized with Re (Yang & Noormets, 2020). We fit the flux-based function using daily cumulative Re (g C m⁻² d⁻¹), here denoted A(t):

$$A(t) = y_0 + a_1/[1 + \exp(-(t - t_{01})/b_1)^{c_1}] - a_2/[1 + \exp(-(t - t_{02})/b_2)^{c_2}],$$
 (1)

where A(t) is daily cumulative Re (g C m⁻² d⁻¹) at day of year (DOY) t (t = 1, ..., 365), and $a_1, a_2, b_1, b_2, c_1, c_2, t_{01}, t_{02}$, and y_0 are empirical fitting parameters (Gu et al., 2003, 2009). As described in Yang and Noormets (2020), y_0 is the dormant season base flux, a_1 and a_2 control the flux magnitude, and b_1, b_2, c_1 , and c_2 are transition and curvature parameters. Equation (2) results in a smooth curve that simultaneously represents the phenophases of growing season initiation and senescence (Gu et al., 2009). Eddy covariance-measured daily cumulative Re data were used to parameterize A(t) for each site and year (Appendix S1: Figures S1–S2, Table S3).

Estimated date of Re-derived VCP using GR approach

The GR method (Gu et al., 2009) of estimating key ecosystem-scale biological events during phenological processes is based on the growth rate of A(t), which is defined by the function k(t) (Gu et al., 2003).

$$k(t) = dA(t)/dt$$

$$= a_1c_1/b_1 \cdot \exp[-(t - t_{01})/b_1]/$$

$$\{1 + \exp[-(t - t_{01})/b_1]\}^{1+c_1}$$

$$-a_2c_2/b_2 \cdot \exp[-(t - t_{02})/b_2]/$$

$$\{1 + \exp[-(t - t_{02})/b_2]\}^{1+c_2}.$$
(2)

After parameterizing A(t) with daily Re, the k(t) function is used to calculate the growth rate of Re (Gu et al., 2003, 2009). Plant greenup and senescence phases during the growing season are defined using the maximum and

minimum values of k(t), and VCP metrics describing the start of respiration, end of respiration, start of peak, day of peak, and end of peak (SOR_{GR}, EOR_{GR}, SOP_{GR}, DOP_{GR}, and EOP_{GR}, respectively; DOY) are found based on peak recovery day and peak senescence day using derived recovery and senescence lines according to Gu et al. (2009) (Figure 2a).

Estimated date of Re-derived VCP using TD approach

The TD method for estimating key ecosystem-scale biological events during phenological processes estimates the dates of these events based on local extrema of the TD of the A(t) function (Gonsamo et al., 2013; Liu et al., 2020). The date of the SOR, for example, is at the intersection of the tangent at the steepest part of the curve and the tangent of the asymptotic start of the fitted curve, which corresponds to the maximum value among the roots of its TD (Gonsamo et al., 2013). Since Gu et al. (2009) did not provide an analytical formula for the TD of A(t), numerical methods are used to estimate partial derivatives of A(t) via the function "diff()" (MATLAB R2014b; MathWorks Inc., Natick, MA). Since A(t)involves one independent variable (t), the derivative is uniquely defined at each value of t (Figure 2b). Using this method, SOR_{TD} is defined as the DOY of the first maximum value of the third derivative, start of peak (SOP_{TD})

is defined as the DOY of the second maximum value of the third derivative, end of peak (EOP_{TD}) is defined as the DOY of the second minimum value of the third derivative, and the end of respiration (EOR_{TD}) is defined as the DOY of the third minimum value of the TD (Gonsamo et al., 2013).

Model framework for VCP metrics

The fitting of the nine-parameter model of interannual Re and the algorithms for Re-derived VCP metrics (GR and TD) were coded and visualized in MATLAB R2014b (MathWorks Inc.). The fit of each annual estimated function was verified by examining the adjusted coefficient of determination (R^2). We judged the model to have good fit when $R^2 > 0.8$. While this minimum value for the fit statistic ensures that these models can explain at least 80% of the variation in Re data, it is worthwhile noting that since the true dates of these events are unknown, no true measure of accuracy or bias can be estimated.

Since the two study sites are evergreen coniferous forests and the annual average air temperature in the subtropical region is relatively high, the growing season may cover the whole year (W. Zhang et al., 2020). This leads to the fitted curve of Re maintaining low amplitude and slope (0.02–0.03 g C m⁻² d⁻¹) during the annual growing season in some cases, and the SOR and EOR of the GR and TD method may extend beyond the annual scale,

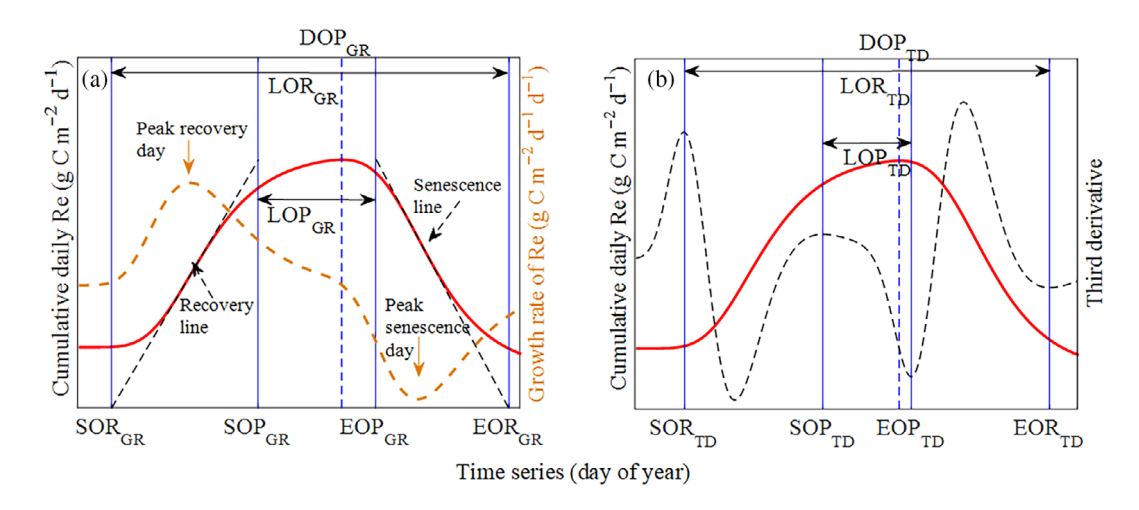


FIGURE 2 Schematic diagram of estimated Re-derived vegetation carbon phenology metrics extracted using: (a) growth rate approach (GR), (b) third derivative approach (TD). A(t) is the fitted red curve, length of respiration (LOR) was defined as the number of days between the start of respiration (SOR) and end of respiration (EOR), the number of days between the start of peak (SOP) and end of peak (EOP) was defined as the length of peak (LOP), and subscripts GR and TD refer to the approach used. In (a), k(t) is the fitted yellow dashed curve, yellow arrows represent extreme values in the daily change of modeled Re (peak recovery and peak senescence), defined by Gu et al. (2009). In (b), the black dashed curve is the third derivative of A(t). Since day of peak (DOP) was uniquely determined by A(t) for each site-year, $DOP_{GR} = DOP_{TD}$

ECOSPHERE 7 of 17

resulting in a negative value of SOR and EOR >365 days. In this case, SOR was corrected to DOY 1 and EOR was corrected to DOY 365 (Appendix S1: Figures S1–S2).

Vegetation greenness phenology from satellite-based remote sensing

In order to examine the relationship between Re-derived VCP and vegetation greenness, we obtained 2009-2017 500-m spatial resolution and yearly interval land surface phenology (LSP) data from the NASA Moderate Resolution Imaging Spectroradiometer (MODIS, https:// ladsweb.modaps.eosdis.nasa.gov/) land cover dynamics products (MCD12Q2 v006) for the two study sites (Friedl et al., 2019). In this spectral-based apparent phenology product, first a QA/QC-weighted penalized cubic smoothing spline is fit to the time series of the 2-band EVI (EVI2); then, the curve's amplitude is used to determine the date of important biological events, including onset of greenup (15% amplitude), mid-greenup (50% amplitude), peak of EVI2, maturity (90% amplitude), senescence (90% amplitude), mid-greendown (50% amplitude), and dormancy (15% amplitude; Friedl et al., 2019). MODIS-derived LSP data were processed with the MODIS Reprojection Tool using ArcGIS (Version 10.2; ESRI) for projection correction, image cropping, and raster calculation. Since the EC flux source area extends 500 m from the towers (Wiesner et al., 2018, 2019), we used the average of the MODIS-derived phenology dates obtained within a 500-m radius circle centered at each EC site. However, we also calculated the minimum and maximum value within the footprint to allow evaluation across the possible range of values obtained from MODIS EVI and further assess relationships between MODIS dates and those of the nine-parameter function.

We defined the onset of greenup as the DOY of the start of the effective growing season (SOES_{EVI2}), maturity as DOY of the start of peak (SOP_{EVI2}), peak as the DOY of peak of EVI2 (DOP_{EVI2}, in days), senescence as the DOY of the end of peak (EOP_{EVI2}, in days), and dormancy as the DOY of the end of the effective growing season (EOES_{EVI2}, in days). The number of days between SOES_{EVI2} and EOES_{EVI2} was defined as the length of the effective growing season (LOES_{EVI2}, in days), and the number of days between SOP_{EVI2} and EOP_{EVI2} was defined as the length of peak (LOP_{EVI2}, in days) (Appendix S1: Figure S3). As with VCP metrics estimated from the nine-parameter function (with either GR or TD method), phenology dates derived from EVI cannot provide evidence of accuracy or precision, since the true values are unknown. However, these estimates provide a useful means for identifying patterns and consistent trends both within and among methods.

Statistical analysis

To compare Re-based VCP metrics derived from the GR and TD approaches, we first examined correlations among estimated LOR, LOP, SOR, SOP, EOP, and EOR values by site and method. To test for significant differences between methods, we used a paired t test with each of the VCP metrics, comparing values derived from the GR and TD methods with an additional fixed effect to account for site. We checked the assumption that prescribed fires (applied in odd-numbered years) did not affect VCP metrics by also fitting models which included a fixed effect for fire; a lack of significant fire effect was taken as verification of this assumption. Using the average MODIS EVI phenology date values within the tower footprint as response variables, we quantified the degree to which Re-based phenology metrics derived from the GR and TD methods were related to phenology dates derived from EVI greenness using similar statistical methods, comparing to both the TD and GR methods in separate models. We then tested the sensitivity of these conclusions by repeating analyses, using the minimum and maximum phenology date values recorded in the tower footprint each year.

To test the relationship between environmental variables and Re-derived VCP metrics, we computed Pearson correlation coefficients, quantifying the relationship between annual VCP metrics for each method (TD and GR) versus average T_a (air temperature), PAR (photosynthetically active radiation), and cumulative Pptn (precipitation). We tested SOR against values of T_a and PAR during spring (March to May) and Pptn during winter (January to March). Start of peak was tested against spring values of T_a , PAR, and Pptn. DOP, EOP, and LOP were tested against early summer (June to August) values of T_a , PAR, and Pptn, whereas EOR was tested against autumn (September to November) values. Length of respiration was tested against annual values of T_a , PAR, and Pptn. Statistical analyses and visualization were processed in OriginPro 9.1 (OriginLab Corporation, Northampton, MA) and R (R Core Team, 2021). Model assumptions of normality and homoscedasticity were visually evaluated.

RESULTS

Application of flux-based function to model the interannual behavior in Re

Fits of the flux-based function by site and year to daily cumulative Re using the A(t) function indicated good agreement, with R^2 values \geq 0.8 (Appendix S1: Table S1). The application of the two algorithmic approaches, in

terms of ability to determine estimated VCP metrics, was consistent at the site level in most years. For example, in 2011, 2012, and 2016, both approaches indicated respiration exceeded the 365-day annual timescale in the xeric site (Table 2). However, there were significant differences in 2017; with the TD approach, SOR_{TD} values were at DOY 21–29, whereas the GR approach values were 45 days earlier (beyond the annual timescale). Due to unusual winter air temperature increases at the mesic site in 2015 and 2016, estimated functional fits under both approaches were uncertain, and the VCP metrics SOR, EOR, and LOR could not be calculated.

Differences in VCP metrics derived from GR and TD methods

In general, the GR method predicted earlier spring (SOR) and later summer (EOP) VCP metrics than the TD method (Figure 3; Table 3). In early spring, the GR method prediction of SOR was 27 days earlier than the TD method. In terms of summer metrics, SOP predicted by the GR method was 14–19 days earlier than the TD, while EOP was 8–11 days earlier (Table 3; Figure 3).

At both sites, the GR method was significantly and positively correlated with the TD method in predicting SOR, SOP, and EOP in each site (p < 0.05; Figure 3). The TD and GR methods were positively correlated for EOR, but not significantly so (p > 0.05). Paired t tests indicated that none of the Re-derived VCP metrics (SOR, SOP, EOP, EOR, LOR, and LOP) were significantly different by site (p > 0.05) (Table 3), but that there were significant differences (p < 0.05) between the two algorithms for all

of the parameters except SOP, which presented weaker evidence of differences between the methods (p = 0.071; Table 3).

On average, values of LOR_{GR} were 58 days longer than that of LOR_{TD} (Table 3). Because average LOP_{GR} was 26 days longer than LOP_{TD} , the TD method predicted a shorter length of Re (in days) and length of the peak (in days) than the GR method in the study land-scape (Figure 4), especially during 2013 and 2014. Prescribed fire had no discernible impact on the

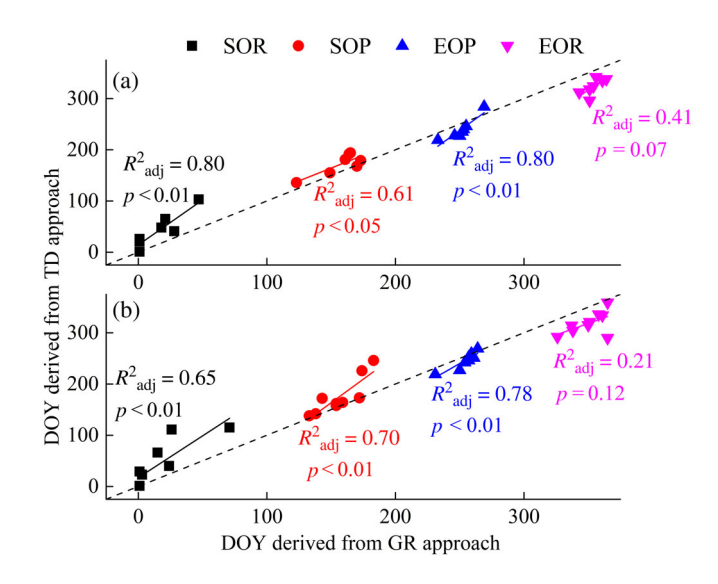


FIGURE 3 Day of year (DOY) of start of respiration (SOR), start of peak (SOP), end of peak (EOP), and end of respiration (EOR) estimated by third derivative (TD) method versus growth rate (GR) method: (a) mesic site, (b) xeric site

TABLE 2 Estimated vegetation carbon phenology metrics start of respiration (SOR), end of respiration (EOR), and length of respiration (LOR) from fitting nine-parameter flux-based function using the growth rate (GR) and third derivative (TD) approach by site and year

| | SOR | | | | EOR | | LOR | | | | | |
|------|----------------|----------------|----------------|----------------|-------|-----|-------|-----|------------------|------------------|------------------|------------------|
| | Mesic | | Xeric | | Mesic | | Xeric | | Mesic | Mesic | | |
| Year | GR | TD | GR | TD | GR | TD | GR | TD | GR | TD | GR | TD |
| 2009 | 47 | 103 | 15 | 66 | 364 | 338 | 361 | 334 | 317 | 235 | 346 | 268 |
| 2010 | 28 | 41 | 24 | 40 | 356 | 342 | 365 | 359 | 328 | 301 | 341 | 319 |
| 2011 | 1 ^a | 1 ^a | 1 ^a | 1 ^a | 351 | 296 | 326 | 292 | 350 ^a | 295 ^a | 325 ^a | 291 ^a |
| 2012 | 1 | 26 | 1 ^a | 1 ^a | 343 | 312 | 337 | 314 | 342 | 286 | 336 ^a | 313 ^a |
| 2013 | 21 | 65 | 71 | 115 | 351 | 318 | 350 | 315 | 330 | 253 | 279 | 200 |
| 2014 | 18 | 48 | 26 | 111 | 354 | 324 | 351 | 321 | 336 | 276 | 325 | 210 |
| 2015 | b | b | 3 | 23 | b | b | 365 | 290 | b | b | 362 | 267 |
| 2016 | b | b | 1 ^a | 1 ^a | b | b | 338 | 304 | b | b | 337 ^a | 303 ^a |
| 2017 | 1 ^a | 21 | 1 ^a | 29 | 361 | 335 | 358 | 336 | 360 | 314 | 357 | 307 |

^aExceeded timescale, indicating that estimated SOR was <1 day, or that EOR/LOR was >365 days.

^bWinter warming caused unstable estimates.

ECOSPHERE 9 of 17

TABLE 3 Estimates, SEs, and *p* values associated with paired *t* test of vegetation carbon phenology (VCP) metrics (EOP, end of peak; EOR, end of respiration; LOP, length of peak; LOR, length of respiration; SOP, the start of peak; SOR, start of respiration) as a function of phenology metric extraction algorithm (GR, growth rate; TD, third derivative) and site

| | Estimate | | SE | | p | | |
|------------|------------------------|----------------------|-----------|-------|-----------|-------|--|
| VCP metric | GR versus TD algorithm | Xeric vs. mesic site | Algorithm | Site | Algorithm | Site | |
| SOR | -26.86 | -0.25 | 9.42 | 12.57 | 0.013 | 0.984 | |
| SOP | -14.29 | -4.71 | 7.32 | 9.76 | 0.071 | 0.637 | |
| EOP | 11.29 | -3.29 | 3.85 | 5.13 | 0.011 | 0.532 | |
| EOR | 30.71 | 1.06 | 6.12 | 8.16 | < 0.01 | 0.898 | |
| LOR | 57.57 | 1.32 | 10.71 | 14.28 | < 0.01 | 0.928 | |
| LOP | 25.57 | 1.43 | 7.19 | 9.58 | <0.01 | 0.884 | |

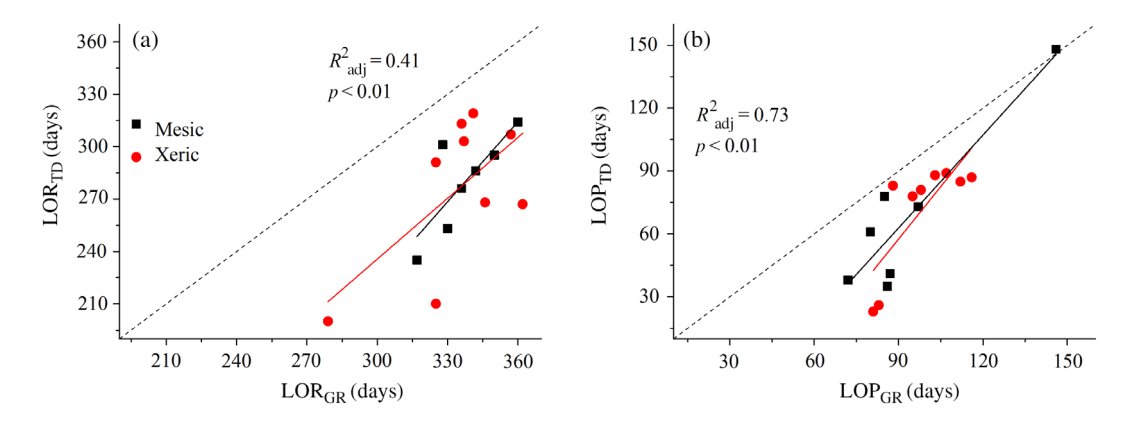


FIGURE 4 Length of respiration (LOR) and length of peak (LOP) estimated by third derivative (TD) versus growth rate (GR) methods by site: (a) LOR_{GR} versus LOR_{TD}, (b) LOP_{GR} versus LOP_{TD}

performance of either methods across all estimated VCP metrics (p > 0.33; analysis not shown).

Relationship between VCP metrics and vegetation greenness phenology

DOP estimated from the flux-based function (where estimates are the same under both TD and GR methods) was on average 10 days later than that of MODIS, a difference which was significant (p < 0.001) only when tested against the minimum MODIS values in the tower footprint (Table 4; Appendix S1: Figure S4). Moreover, differences were significantly more pronounced (an additional 25 days later) in the xeric site (p < 0.034); however, this was the only significant site effect across all VCP metrics (data not shown). Only EOP estimates were impacted by prescribed fire; EOP_{EVI2} was 23–39 days earlier during nonfire years versus that of fire years, a difference which was more pronounced in the mesic site (data not shown).

When comparing the other MODIS-derived dates versus that of the flux-based function using the GR algorithm, the average and minimum dates indicated by

MODIS were significantly earlier than the VCP metrics (p < 0.002), except when examining SOP or SOES. While SOP values were not significantly different, SOES_{EVI2} were significantly later than SOR_{GR} (p < 0.001). Using the maximum dates derived from MODIS, all VCP metrics were significantly different from those estimated with the GR method (p < 0.032) except for EOES_{EVI2} versus EOR_{GR} (p = 0.058). Using the GR method, LOR_{GR} was on average 98 days longer than LOES_{EVI2}, while LOP_{GR} was on average 38 days longer than LOP_{EVI2} (Figure 5).

MODIS-derived dates were generally closer to those indicated by the TD method. There were no significant differences between SOP, EOR, and LOP from the TD method and that of MODIS (for average, minimum and maximum; p > 0.096; Table 4). When considering average, minimum, and maximum values, SOES_{EVI2} values were later than those of SOR_{TD}, and LOES_{EVI2} values were shorter than LOR_{TD} values. For EOP, MODIS values only differed from the TD dates when considering the maximum values. Using the TD method, LOR_{TD} was on average 40 days longer than LOES_{EVI2}, while LOP_{TD} was on average 13 days longer than LOP_{EVI2} (and not significantly different; Figure 5).

TABLE 4 Estimates and *p* values associated with paired *t* test of MODIS-derived phenological dates (average, minimum, and maximum values in flux footprint) versus estimated vegetation carbon phenology (VCP) metrics (DOP, day of peak; EOES, end of effective growing season; EOP, end of peak; EOR, end of respiration; LOES, length of effective growing season; LOP, length of peak; LOR, length of respiration; SOES, start of effective growing season; SOP, the start of peak; SOR, start of respiration), for each phenology metric extraction algorithm (GR, growth rate; TD, third derivative)

| | | Estimate | | | p | | |
|------------|-----------------|----------|--------|--------|---------|---------|---------|
| Comparison | VCP metric | Avg. | Min | Max | Avg. | Min | Max |
| Versus GR | DOP | -10.15 | -30.78 | 9.67 | 0.096 | < 0.001 | 0.188 |
| | SOES versus SOR | 70.14 | 62.71 | 75.57 | < 0.001 | < 0.001 | < 0.001 |
| | SOP | 5.90 | -7.57 | 20.71 | 0.324 | 0.288 | 0.032 |
| | EOP | -32.33 | -44.29 | -14.00 | 0.001 | < 0.001 | 0.011 |
| | EOES versus EOR | -27.76 | -42.29 | -16.00 | 0.002 | < 0.001 | 0.058 |
| | LOES versus LOR | -97.90 | -105.0 | -91.57 | < 0.001 | < 0.001 | < 0.001 |
| | LOP | -38.24 | -36.71 | -34.71 | 0.001 | 0.004 | 0.001 |
| Versus TD | DOP | -10.15 | -30.78 | 9.67 | 0.096 | < 0.001 | 0.188 |
| | SOES versus SOR | 43.29 | 35.86 | 48.71 | 0.009 | 0.024 | 0.005 |
| | SOP | -8.38 | -21.86 | 6.43 | 0.439 | 0.095 | 0.588 |
| | EOP | -21.05 | -33.00 | -2.71 | 0.040 | 0.005 | 0.660 |
| | EOES versus EOR | 2.95 | -11.57 | 14.71 | 0.758 | 0.217 | 0.152 |
| | LOES versus LOR | -40.33 | -47.43 | -34.00 | 0.010 | 0.005 | 0.028 |
| | LOP | -12.67 | -11.14 | -9.14 | 0.402 | 0.500 | 0.474 |

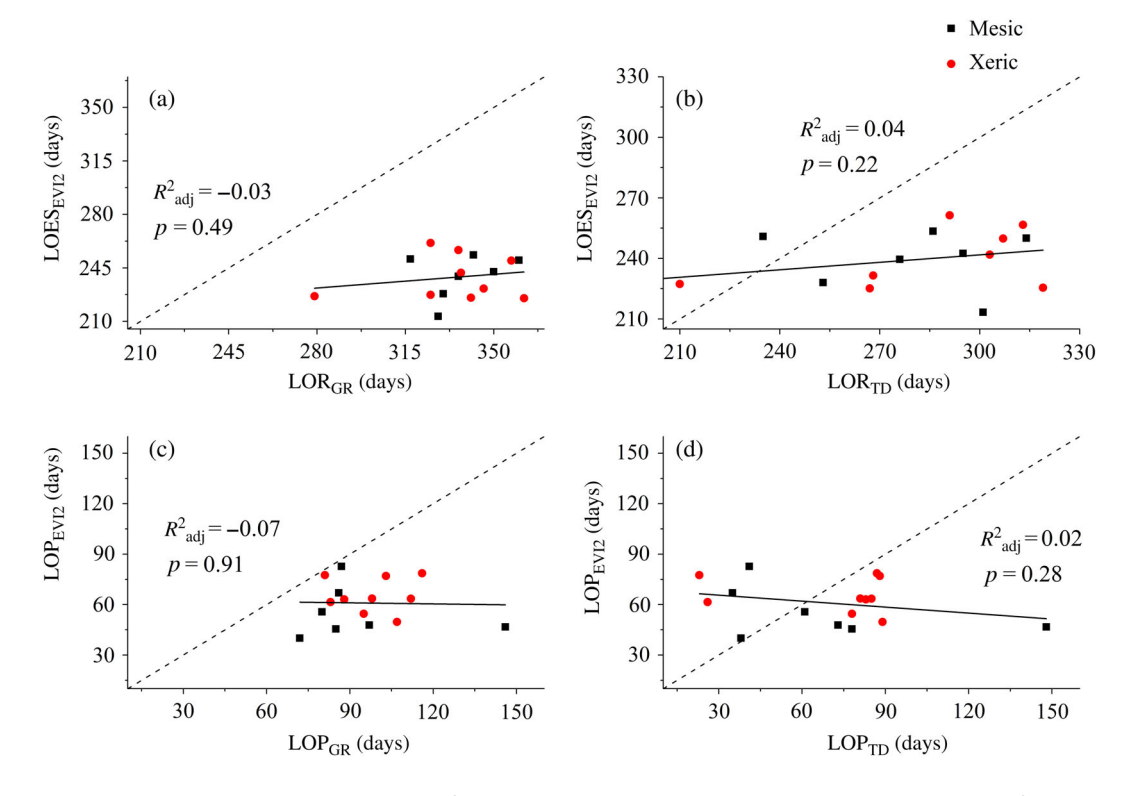


FIGURE 5 Vegetation greenness phenology derived from MODIS EVI using the average value within the tower footprint, versus those of vegetation carbon phenology (VCP) by site: MODIS EVI-derived length of effective season (LOES_{EVI2}) versus VCP length of respiration (LOR) derived using (a) the growth rate method (LOR_{GR}) and (b) the third derivative method (LOR_{TD}), MODIS EVI-derived length of peak (LOP_{EVI2}) versus VCP length of peak (LOP) derived using (c) the growth rate method (LOP_{GR}) and (d) the third derivative method (LOP_{TD})

ECOSPHERE 11 of 17

TABLE 5 Pearson correlation coefficient between time series of environmental variables: $T_{\rm a}$ (air temperature), PAR (photosynthetically active radiation), and Pptn (precipitation) versus vegetation carbon phenology metrics (DOP, day of peak; EOP, end of peak; EOR, end of respiration; LOP, length of peak; LOR, length of respiration; SOP, the start of peak; SOR, start of respiration)

| | Mesic si | ite | | | | | Xeric site | e | | | | |
|--------|------------------|-------|-------|------------------|-------|---------|------------------|-------|--------|------------------|-------|---------|
| | GR approach | | | TD app | roach | | GR approach | | | TD approach | | |
| Metric | $\overline{T_a}$ | PAR | Pptn | $\overline{T_a}$ | PAR | Pptn | $\overline{T_a}$ | PAR | Pptn | $\overline{T_a}$ | PAR | Pptn |
| SOR | -0.53 | -0.06 | 0.43 | -0.53 | -0.34 | 0.64 | -0.84** | -0.01 | 0.76** | -0.91** | -0.02 | 0.66* |
| SOP | -0.62 | -0.29 | -0.05 | -0.60 | -0.27 | -0.06 | 0.28 | 0.04 | 0.17 | 0.51 | 0.18 | 0.04 |
| DOP | -0.05 | -0.09 | 0.11 | -0.05 | -0.09 | 0.11 | 0.32 | 0.18 | 0.26 | 0.32 | 0.18 | 0.26 |
| EOP | -0.78* | -0.6 | 0.48 | -0.61 | -0.51 | 0.44 | -0.14 | -0.29 | 0.12 | -0.19 | 0.07 | -0.45 |
| EOR | 0.53 | 0.24 | 0.25 | 0.63 | -0.35 | 0.22 | 0.12 | -0.28 | 0.51 | 0.25 | -0.36 | 0.03 |
| LOR | 0.77* | 0.23 | -0.65 | 0.50 | 0.58 | -0.81** | 0.40 | -0.06 | -0.48 | 0.62 | 0.43 | -0.78** |
| LOP | -0.28 | -0.19 | 0.18 | -0.36 | -0.36 | 0.34 | 0.58 | 0.47 | -0.09 | 0.15 | 0.08 | 0.09 |

Note: SOR is tested against spring (March to May) values of T_a and PAR, and winter (January to March) Pptn. SOP is tested against spring values of T_a , PAR, and Pptn. DOP, EOP, and LOP are tested against summer (June to August) values of T_a , PAR, and Pptn. EOR is tested against autumn (September to November) values of T_a , PAR, and Pptn. LOR is tested against annual values of T_a , PAR, and Pptn. *p < 0.05; **p < 0.01.

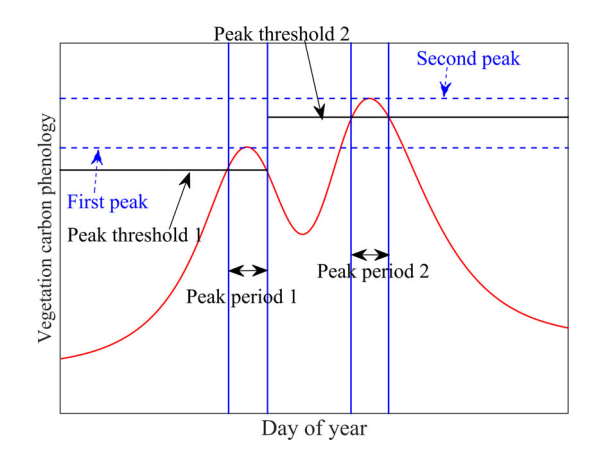


FIGURE 6 Conceptual diagram of peak period estimation for multi-peak behavior in vegetation carbon phenology. The blue dashed lines mark the multiple peak values, and the black solid lines mark individualized amplitude thresholds based on each peak. The solid blue lines represent estimate of the start and end of the peak periods derived from each peak threshold.

Relationship between environmental variables and re-derived VCP metrics

Correlation analyses of Re-derived VCP metrics versus environmental variables indicated differences between the GR and TD approaches and sites (Table 5). EOP_{GR} of the mesic site was sensitive to $T_{\rm a}$ (R=-0.78, p<0.05); with increased summer $T_{\rm a}$, the peak period of Re ended earlier. SOR_{GR} of the xeric site was sensitive to spring $T_{\rm a}$ (R=-0.84, p<0.01) and winter precipitation (R=0.76, p<0.01); as spring $T_{\rm a}$ increased, Re was activated earlier and increased precipitation delayed the start of Re. In the

xeric site, the response of SOR_{TD} to spring T_a and winter precipitation was consistent with that of SOR_{GR} .

On the annual scale, the LOR_{GR} of the mesic site was also sensitive to $T_{\rm a}$ (R=0.77, p<0.05); as $T_{\rm a}$ increased, Re was prolonged. LOR_{TD} of both sites was sensitive to precipitation (R=-0.8, p<0.01); the period of Re was shortened when precipitation increased.

In general, the VCP metrics derived from GR and TD approaches were different in response to precipitation and T_a by site, especially LOR. The xeric site may be more sensitive to environmental dynamics in spring (i.e., SOR), while the mesic site may be more sensitive to environmental dynamics during early summer (i.e., EOP).

DISCUSSION

In this study, we used EC and remote sensing products, and fit a model of interannual Re to determine biological event dates. Our results indicate that the algorithm used to determine the date of VCP metrics can have a significant impact on the estimated phenophases of Re (Wu et al., 2017). Under both approaches, spring phenology (SOR) and LOR were highly sensitive to winter precipitation and air temperature (Table 5), similar to Kross et al. (2014). This effect may be exacerbated with higher average air temperatures in subtropical regions where the evergreen canopy is active most of the year (Whelan et al., 2013), which causes uncertainty in the signal of phenophase transition. Furthermore, warmer winters and higher water availability in summer had a significant impact on estimating VCP metrics for Re, as variation in Re leads to prolonged growing season and multi-peak

behavior in summer (Younes et al., 2020). In addition, we found that the date of fall senescence derived from the 2-band EVI was often mismatched with modeled Re (p < 0.01) (Appendix S1: Figure S4), in agreement with Wu et al. (2014). However, 2-band EVI and its derived phenology products may not be sufficient to predict VCP in subtropical evergreen coniferous forests (Wu et al., 2014, 2017), as low variation in canopy greenness due to the evergreen canopy may obscure identification of phenological event dates. Only the start of the peak period (maximum) of vegetation greenness was synchronized, agreeing with VCP metrics from the flux-based model.

Influence of phenological metric extraction algorithm on phenophase transition

We found that phenological extraction algorithms (GR and TD approach) differed significantly in their estimates of Re-based VCP metrics (Gong et al., 2020; Wu et al., 2017; Zhou, 2018) (Table 2). Compared to temperate ecosystems, these subtropical ecosystems have higher annual average air and soil temperatures (Whelan et al., 2013), which is also associated with smaller interannual amplitude of Re; that is, there are relatively small changes in the slope of day-to-day carbon dynamics (W. Zhang et al., 2020). This causes a less abrupt spring recovery and autumn senescence than higher latitude ecosystems (Gu et al., 2009; W. Zhang et al., 2020). A larger buffer zone is formed during the phenophase transition, which results in significantly shorter LOR and LOP (length of the peak respiration) from the TD method versus that of the GR method. Since the phenological date given by the GR method uses a dynamic threshold based on the maximum rate of recovery and senescence rather than the local extrema in the TD of modeled Re (Zhou, 2018), this includes a part of the buffer zone and the GR method may cover more phenological signals than the TD method. These differences may be attributed to the fact that the TD method identifies the precise location of the inflection point in the phenology behavior, and the boundary of the phenophase is clear. This method will have better performance and accuracy in areas with strong seasonal differences. While the GR method relies on the differences in vegetation development rates between spring and autumn, using the parameterized function to identify the overall trend between adjacent phenophases, rather than the timing of specific inflection points, results in higher flexibility in determining phenological dates (Zhou, 2018), which may be more applicable in subtropical regions. To adequately assess the sensitivity of the phenological extraction algorithm

mechanism to the phenological signals of sites in different climate zones, more long-term, multisite integrated analysis is needed to provide a wider range of parameter estimates for the model (Wu et al., 2017).

It is also worth noting that prescribed fire is applied to the study site in odd-numbered years in early spring (Starr et al., 2016), which may also cause uncertainty in the determination of SOR with both the GR and TD approach. Indeed, 2011, in which both GR and TD methods indicated a negative value for SOR and in 2017, in which the GR method indicated a negative value for SOR, were burn years. Prescribed fire has been found to have a significant, but short-term impact on the carbon dynamics at the site in early spring (Starr et al., 2015). However, we found no clear pattern in our results in terms of differences in estimated VCP metrics in fire versus nonfire years, except when considering the difference between MODIS-derived EOP and those estimated from the flux-based models, leading us to conclude that additional years of observation are required to detect differences in VCP metrics due to prescribed fire.

Site differences in Re-derived VCP metrics

Even with the same phenology metric extraction algorithm, we found that the Re-derived dates may be very different by site. Taking 2012 as an example, the SOP_{GR} of the mesic site was estimated at DOY 123, whereas the SOP_{GR} of the xeric site was 60 days later (DOY 183). The main reason for this phenomenon was the site-level spring increase in physiological activity. The spring of the mesic site was recovery rate $(0.05~g~C~m^{-2}~d^{-1})$ than that of the xeric site (0.03 g C m⁻² d⁻¹), which led the mesic site to reach the peak period earlier (SOP) (Appendix S1: Figures S1-S2). Similarly in 2013, due to a more rapid increase in Re at the xeric site (0.08 g C m⁻² d⁻¹), it reached the peak period earlier than the mesic site (0.04 g C m $^{-2}$ d $^{-1}$). Similar patterns in these sites resulted using the TD method in 2012-2013 (Appendix S1: Figures S1-S2). Thus, differences in estimated VCP metrics by year go beyond the choice of phenological extraction algorithm. Differences in site-level flux development rates in spring/ autumn can lead to large differences in site-level phenological dates (Gu et al., 2009).

The differences in phenology observed in this study may be attributed to the ecosystems' responses to varying environmental conditions caused by site-level heterogeneity. In some years, the higher dominance of conifer species at the mesic site may have led to broader peaks (longer Re season), whereas the presence of more hardwood trees at the xeric site led to earlier leaf-out, before ECOSPHERE 13 of 17

beginning a steep peak and shorter season. The spring phenology (SOR) of the more oak-dominated xeric site was more sensitive to air temperature and winter precipitation, as warming in spring induces an earlier greening of the understory (H. Wang et al., 2019). However, increases in winter precipitation delayed SOR, which may be related to a reduction of radiation that drives carbon capture and ultimately Re. The mesic site's spring phenology was less sensitive to air temperature and precipitation, which may be due to its higher abundance of understory plants and evergreen trees (Whelan et al., 2013), which contribute ecosystem phenological signals in early spring. By contrast, the xeric site has a lower density of understory plants, which may limit the ecosystem phenological signals. Nonetheless, using the GR method, we found that the mesic site's end of peak Re (EOP_{GR}) was abbreviated with higher summer temperatures, while its length (LORGR) was prolonged with higher annual temperatures. This observed phenomenon may be a consequence of the general site pattern, where years with warmer summer temperatures tended to have lower winter temperatures over our 9 years of observation (R = -0.61). As climate change creates more seasonal variation in temperature, these results suggest that the GR method for estimating VCP metrics is more sensitive to this variability and timing of seasonal patterns.

Mismatch between vegetation greenness and VCP in evergreen coniferous forests

Remote sensing products are widely used to characterize the phenology of vegetation and for cross-validation with EC-based VCP (Atkinson et al., 2012; Bórnez et al., 2020; Gonsamo et al., 2012). In this study, among the VCP metrics, only Re-derived DOP and SOP were well-matched with vegetation greenness for both methods, while EOES and LOP showed correlations with TD (Table 4, Appendix S1: Figure S4). This may be because the productivity of evergreen species in these study sites does not depend as strongly on leaf production compared to deciduous forests (Wu et al., 2014, 2017); coupled with the two-year needle replacement cycle, the greenness of needles cannot fully predict the seasonal pattern of VCP (Wu et al., 2014, 2017). Instead, medium- and/or longterm weather changes induced by climate change, such as photoperiod in spring and air temperature in summer, may contribute more to VCP dynamics of these forest (Gong et al., 2021; Kong et al., 2020; Wu et al., 2014). In addition, due to the 8-day remote sensing data cycle and limited spatial resolution, some LSP signals may be missed or delayed by the satellite sensors. Moreover, the MODIS MCD12Q2 product relies on fitted cubic splines

and fixed amplitude thresholds to determine LSP metrics, which may also have affected our results (Younes et al., 2021). While our uncertainty analysis using the maximum and minimum values across the tower footprint showed consistent results across space, we did not account for this temporal uncertainty. Thus, there is the potential for asynchrony of vegetation greenness and VCP in evergreen coniferous forests (Kong et al., 2020). Other satellite-derived indexes such as solar-induced chlorophyll fluorescence (SIF) may perform better then EVI for identifying phenological transitions, though Zhang et al. (2022) showed that uncertainty in identifying phenological dates was similar for EVI and SIF.

Short-term and long-term weather anomalies

The carbon exchange between longleaf pine ecosystems and the atmosphere is affected by weather variables such temperature and precipitation et al., 2013). In 2015 and 2016 at the mesic site, we observed an increase in winter Re, which caused uncertainty in estimated VCP metrics. Since winter Re was greater than that in spring, the estimated dates of EOR extended beyond DOY 365, in both GR and TD algorithms (Appendix S1: Figure S5). The abnormal increase in Re at the mesic site during these two winters was mainly due to warmer air temperatures from November and December of these years, which was 2.2 and 3.8°C higher than normal. Since the winter warming rate of 2015 was higher than that in 2016, this also led to a higher growth rate of Re in the winter of 2015. This warming caused an abnormal phenology phenomenon where Re increased for a second time during that year (i. e., two values of SOR), which caused an insignificant signal for EOR. While the xeric site also experienced abnormal winter warming, the phenological model of Re was still able to yield an estimate for EOR. This difference in phenological response could be a consequence of the site's forest structure and species composition (Wiesner et al., 2020, 2021). As climate change has given rise to more pronounced winter warming at mid-latitudes, and winter warming has been shown to impact Re more than summer warming (Kreyling et al., 2019), this result points to the need for models and methods that can account for shifts in weather extremes.

During summer, variation in Re may be caused by site-level water availability (Starr et al., 2016; Wiesner et al., 2018, 2019), which also adds uncertainty in the timing of SOP and EOP. These fluctuations cause the growth rate of Re to appear as multiple peaks in summer (Appendix S1: Figures S1–S2), and the GR and TD

method may not give a biologically reasonable LOP (Appendix S1: Figure S6). Moreover, when multi-peak behavior occurs, the TD method may predict a shorter LOP compared to the GR method. In the three cases, we reported such abnormal behavior, the default LOP prediction from the GR method overestimated Re, while the default LOP prediction from the TD method underestimated Re (Appendix S1: Figure S6). However, water did not affect DOP (Gong et al., 2021; Gu et al., 2009).

Autumn phenology was also affected by drought. Starting in 2010, severe drought occurred at both sites (Starr et al., 2016). When considering all years, EOR showed no significant association with environmental variables (Table 5); however, if we exclude 2010 data, the negative correlation between EOR_{GR} of the xeric site and autumn radiation becomes significant (R = -0.9, p < 0.01; data not shown), indicating that increases in radiation led to earlier EOR. This may indicate that the respiration rate in autumn was mainly regulated by ecosystem productivity, similar to results reported by Gonsamo et al. (2015).

Limitations and outlook

Short-term weather anomalies from global climate change may become more frequent, and these will have a significant impact on carbon exchange between the ecosystem and the atmosphere (Hutyra et al., 2007; Lian et al., 2021). These day-to-day carbon exchange anomalies will be reflected in phenological modeling, that is, causing multiple peaks in the phenophases during the growing season (Appendix S1: Figures S1-S2). This will make the traditional functions assuming single-peak seasonal dynamics unable to adequately characterize phenological patterns, that is, overestimating underestimating the length of the active season (Younes et al., 2020; Zhou, 2018). While the functional form and phenological metric extraction algorithms tested in this study assume unimodal behavior, extraction methods based on curvature, fixed thresholds, or dynamic thresholds may be more suitable for stable ecosystems (Younes et al., 2020; Zhou, 2018). A potential solution to shortterm summer weather anomalies such as the prediction of peak period (Table 1; Appendix S1: Figures S1–S2) could be determining the length of the peak period based on the amplitude before and after the peak, that is, set thresholds for multiple peak periods based on each peak value, as the DOP is a unique value. This approach may give an approximate estimate of peak length for multipeak behavior in VCP (Figure 6). Yet, such methods may not be able to yield a generalizable function, since it will need to adapt to local conditions and scientific

knowledge (Wu et al., 2017; Younes et al., 2020; Zhou, 2018). In addition, increasing temperatures, which are predicted for many regions globally, may lead to more uncertainty.

The study of anomalies in the carbon exchange between the ecosystem and the atmosphere due to climate change is an area of research concern. However, the coupling process between vegetation phenology, weather, and microclimate is not well understood. This study also explored the relationship between vegetation greenness of subtropical coniferous forests and VCP, but it did not quantify the impact of climate change on vegetation greenness phenology. Moreover, to deal with short-term day-to-day carbon exchange abnormalities, the coupling relationship between vegetation phenology and short-term weather abnormalities should be further studied in conjunction with physiological models (Younes et al., 2020). In addition, the sensitivity of the phenology metric extraction algorithm to climate change has not been fully explored in this study. Although we have quantified the differences between algorithms over 9 years and their relationships to environmental conditions, the uncertainty of VCP response to climate change induced by choice of extraction algorithm needs additional attention. When evaluating phenology at the sitelevel, rigorous model tests and field visits are required (Velasco, 2018), as found by Wu et al. (2017) in a largescale analysis of remote sensing data and ground observations.

CONCLUSION

Our results pointed out that the growth rate method of estimating VCP metrics may be more suitable for modeling subtropical forests due to its sensitivity to temperature, while the TD approach may be better able to distinguish extreme weather anomalies. Winter warming can cause Re to be activated again, and the dynamics of summer water availability can significantly affect the summer phenological process. We found a negative correlation between vegetation greenness and VCP in autumn; thus, spectral-based remote sensing vegetation index products may not have the potential to predict the variability of seasonal carbon dynamics in subtropical evergreen coniferous forests. Finally, although our preliminary results showed variation in VCP metrics derived using parametric methods, models which capture interannual seasonal dynamics have the potential to be applied in the future, as they better describe vegetation growth carryover and changes in vegetation responses to these anomalies, as compared to satellite data (Lian et al., 2021). This finding underlines the need for

ECOSPHERE 15 of 17

additional research, in particular in light of the potential for climate change to alter the systems and increase uncertainty during seasonal transitions.

ACKNOWLEDGMENTS

Yuan Gong and Yinlong Zhang were funded by the National Key Research and Development Program of China (No. 2016YFC0502704) and the Priority Academic Program Development of Jiangsu Higher Education Institutions (PAPD). Christina L. Staudhammer and Gregory Starr acknowledged support from the US National Science Foundation (DEB EF-1241881). Christina L. Staudhammer also acknowledges support from the U.S. National Science Foundation (DEB EF-1702029). All eddy covariance data used in this study are available at: ameriflux.lbl.gov.

CONFLICT OF INTEREST

The authors declare no conflict of interest.

DATA AVAILABILITY STATEMENT

Data from the mesic site (Starr, 2021a) are available from AmeriFlux US-LL1: https://doi.org/10.17190/AMF/1773395. Data from the xeric site (Starr, 2021b) are available from AmeriFlux US-LL3: https://doi.org/10.17190/AMF/1773397.

ORCID

Yuan Gong https://orcid.org/0000-0002-1338-2939 Christina L. Staudhammer https://orcid.org/0000-0003-1887-418X

Gregory Starr https://orcid.org/0000-0002-7918-242X

REFERENCES

- Aber, J., R. P. Neilson, S. McNulty, J. M. Lenihan, D. Bachelet, and R. J. Drapek. 2001. "Forest Processes and Global Environmental Change: Predicting the Effects of Individual and Multiple Stressors." *Bioscience* 51(9): 735–51.
- Atkinson, P. M., C. Jeganathan, J. Dash, and C. Atzberger. 2012. "Inter-Comparison of Four Models for Smoothing Satellite Sensor Time-Series Data to Estimate Vegetation Phenology." Remote Sensing of Environment 123: 400–17.
- Baldocchi, D. 2008. "'Breathing' of the Terrestrial Biosphere: Lessons Learned from a Global Network of Carbon Dioxide Flux Measurement Systems." *Australian Journal of Botany* 56(1): 1–26.
- Baldocchi, D. 2003. "Assessing the Eddy Covariance Technique for Evaluating Carbon Dioxide Exchange Rates of Ecosystems: Past, Present and Future." *Global Change Biology* 9(4): 479–92.
- Berra, E. F., and R. Gaulton. 2021. "Remote Sensing of Temperate and Boreal Forest Phenology: A Review of Progress, Challenges and Opportunities in the Intercomparison of In-Situ

- and Satellite Phenological Metrics." Forest Ecology and Management 480: 118663.
- Bórnez, K., A. Descals, A. Verger, and J. Peñuelas. 2020. "Land Surface Phenology from VEGETATION and PROBA-V Data. Assessment over Deciduous Forests." *International Journal of Applied Earth Observation and Geoinformation* 84: 101974.
- Friedl, M., J. Gray, and D. Sulla-Menashe. 2019. "MCD12Q2 MODIS/Terra+Aqua Land Cover Dynamics Yearly L3 Global 500 m SIN Grid V006 [Data set]." NASA EOSDIS Land Processes DAAC. October 10, 2020. https://doi.org/10.5067/MODIS/MCD12Q2.006.
- García-Oliva, F., and V. J. Jaramillo. 2011. "Impact of Anthropogenic Transformation of Seasonally Dry Tropical Forests on Ecosystem Biogeochemical Processes." In Seasonally Dry Tropical Forests 159–72. Washington, DC: Island Press.
- Goebel, P. C., B. J. Palik, L. K. Kirkman, and L. West. 1997. Field Guide: Landscape Ecosystem Types of Ichauway. Report number 97–1. Newton, GA: Joseph W. Jones Ecological Research Center at Ichauway.
- Gong, Y., and Y. Zhang. 2020. "Characteristics of CO₂ Flux over a Temperate Mixed Forest Ecosystem and Its Response to Air Temperature." *Journal of Northeast Forestry University* 48(5): 40–4+87. https://doi.org/10.13759/j.cnki.dlxb.2020.05.008.
- Gong, Y., Z. J. Guo, K. D. Zhang, L. Xu, Y. Y. Wei, and M. Zhao. 2019. "Impact of Vegetation on CO₂ Flux of a Subtropical Urban Ecosystem." Acta Ecologica Sinica 39(2): 530–41.
- Gong, Y., X. Ji, Y. Hua, Y. Zhang, and N. Li. 2020. "Research Progress of CO₂ Flux in Forest Ecosystem Based on Eddy Covariance Technique: A Review." *Journal of Zhejiang A&F University* 37(3): 593–604. https://doi.org/10.11833/j.issn.2095-0756.20190412.
- Gong, Y., C. L. Staudhammer, S. Wiesner, G. Starr, and Y. Zhang. 2021. "Characterizing Growing Season Length of Subtropical Coniferous Forests with a Phenological Model." *Forests* 12 (1): 95.
- Gonsamo, A., J. M. Chen, and P. D'Odorico. 2013. "Deriving Land Surface Phenology Indicators from CO₂ Eddy Covariance Measurements." Ecological Indicators 29: 203–7.
- Gonsamo, A., J. M. Chen, D. T. Price, W. A. Kurz, and C. Wu. 2012. "Land Surface Phenology from Optical Satellite Measurement and CO₂ Eddy Covariance Technique." *Journal of Geophysical Research – Biogeosciences* 117(G3): G03032.
- Gonsamo, A., H. Croft, J. M. Chen, C. Wu, N. Froelich, and R. M. Staebler. 2015. "Radiation Contributed More than Temperature to Increased Decadal Autumn and Annual Carbon Uptake of Two Eastern North America Mature Forests." Agricultural and Forest Meteorology 201: 8–16.
- Griscom, B. W., J. Adams, P. W. Ellis, R. A. Houghton, G. Lomax, D. A. Miteva, W. H. Schlesinger, et al. 2017. "Natural climate solutions." *Proceedings of the National Academy of Sciences* 114 (44): 11645–50.
- Gu, L., W. M. Post, D. Baldocchi, T. A. Black, S. B. Verma, T. Vesala, and S. C. Wofsy. 2003. "Phenology of Vegetation Photosynthesis." In *Phenology: An Integrative Environmental Science*, edited by M. Schwartz, 467–85. New York: Springer.
- Gu, L., W. M. Post, D. D. Baldocchi, T. A. Black, A. E. Suyker, S. B. Verma, T. Vasala, and S. C. Wofsy. 2009. "Characterizing the Seasonal Dynamics of Plant Community Photosynthesis across a Range of Vegetation Types." In *Phenology of Ecosystem*

Processes 35–58. New York: Springer. https://doi.org/10.1007/978-1-4419-0026-5_2.

- Hutyra, L. R., J. W. Munger, S. R. Saleska, E. Gottlieb, B. C. Daube,
 A. L. Dunn, D. F. Amaral, P. B. de Camargo, and S. C. Wofsy.
 2007. "Seasonal Controls on the Exchange of Carbon and Water in an Amazonian Rain Forest." *Journal of Geophysical Research Biogeosciences* 112(G3): G03008.
- Jin, J., W. Zhan, Y. Wang, B. Gu, W. Wang, H. Jiang, X. Lu, and X. Zhang. 2017. "Water Use Efficiency in Response to Interannual Variations in Flux-Based Photosynthetic Onset in Temperate Deciduous Broadleaf Forests." *Ecological Indicators* 79: 122–7.
- Jones, C. D., P. Cox, and C. Huntingford. 2003. "Uncertainty in Climate Carbon-Cycle Projections Associated with the Sensitivity of Soil Respiration to Temperature." *Tellus Series B: Chemical and Physical Meteorology* 55(2): 642–8.
- Kirilenko, A. P., and R. A. Sedjo. 2007. "Climate Change Impacts on Forestry." *Proceedings of the National Academy of Sciences* 104(50): 19697–702.
- Kirkman, L. K., A. Barnett, B. W. Williams, J. K. Hiers, S. M. Pokswinski, and R. J. Mitchell. 2013. "A Dynamic Reference Model: A Framework for Assessing Biodiversity Restoration Goals in a Fire-Dependent Ecosystem." *Ecological Applications* 23(7): 1574–87.
- Kreyling, J., K. Grant, V. Hammerl, M. A. Arfin-Khan, A. V. Malyshev, J. Peñuelas, K. Pritsch, et al. 2019. "Winter Warming Is Ecologically more Relevant than Summer Warming in a Cool-Temperate Grassland." Scientific Reports 9 (1): 1–9.
- Kross, A. S., N. T. Roulet, T. R. Moore, P. M. Lafleur, E. R. Humphreys, J. W. Seaquist, L. B. Flanagan, and M. Aurela. 2014. "Phenology and its Role in Carbon Dioxide Exchange Processes in Northern Peatlands." *Journal of Geophysical Research Biogeosciences* 119(7): 1370–84.
- Kong, D., Y. Zhang, D. Wang, J. Chen, and X. Gu. 2020. "Photoperiod Explains the Asynchronization between Vegetation Carbon Phenology and Vegetation Greenness Phenology." *Journal of Geophysical Research Biogeosciences* 125(8): e2020JG005636.
- Lian, X., S. Piao, A. Chen, K. Wang, X. Li, W. Buermann, C. Huntingford, J. Peñuelas, H. Xu, and R. B. Myneni. 2021. "Seasonal Biological Carryover Dominates Northern Vegetation Growth." *Nature Communications* 12(1): 1–10.
- Liu, Y., C. Wu, O. Sonnentag, A. R. Desai, and J. Wang. 2020. "Using the Red Chromatic Coordinate to Characterize the Phenology of Forest Canopy Photosynthesis." *Agricultural and Forest Meteorology* 285: 107910.
- Liu, Y., C. Wu, L. Liu, C. Gu, T. A. Black, R. S. Jassal, L. Hörtnagl, et al. 2021. "Interannual and Spatial Variability of Net Ecosystem Production in Forests Explained by an Integrated Physiological Indicator in Summer." *Ecological Indicators* 129: 107982.
- Lloyd, J., and J. A. Taylor. 1994. "On the Temperature Dependence of Soil Respiration." *Functional Ecology* 8(3): 315–23.
- Luo, Q., J. Song, L. Yang, and J. Wang. 2019. "Improved Spring Vegetation Phenology Calculation Method Using a Coupled Model and Anomalous Point Detection." *Remote Sensing* 11(12): 1432. https://doi.org/10.3390/ rs11121432.

- Niu, S., Y. Fu, L. Gu, and Y. Luo. 2013. "Temperature Sensitivity of Canopy Photosynthesis Phenology in Northern Ecosystems." In *Phenology: An Integrative Environmental Science* 503–19. Dordrecht: Springer.
- Noormets, A., J. Chen, L. Gu, and A. Desai. 2009. "The Phenology of Gross Ecosystem Productivity and Ecosystem Respiration in Temperate Hardwood and Conifer Chronosequences." In *Phenology of Ecosystem Processes* 59–85. New York, NY: Springer.
- R Core Team. 2021. R: A Language and Environment for Statistical Computing. Vienna, Austria: R Foundation for Statistical Computing.
- Starr, G., C. L. Staudhammer, H. W. Loescher, R. Mitchell, A. Whelan, J. K. Hiers, and J. J. O'Brien. 2015. "Time Series Analysis of Forest Carbon Dynamics: Recovery of *Pinus palustris* Physiology Following a Prescribed Fire." New Forests 46(1): 63–90
- Starr, G., C. L. Staudhammer, S. Wiesner, S. Kunwor, H. W. Loescher, A. F. Baron, A. Whelan, R. J. Mitchell, and L. Boring. 2016. "Carbon Dynamics of *Pinus palustris* Ecosystems Following Drought." *Forests* 7(5): 98.
- Starr, G. 2021a. "AmeriFlux BASE US-LL1 Longleaf Pine Baker (Mesic site), Ver. 2-5, AmeriFlux AMP, (Dataset)." https://doi. org/10.17190/AMF/1773395.
- Starr, G. 2021b. "AmeriFlux BASE US-LL3 Longleaf Pine Red Dirt (Xeric site), Ver. 1-5, AmeriFlux AMP, (Dataset)." https://doi.org/10.17190/AMF/1773397.
- Velasco, E. 2018. "Go to Field, Look Around, Measure and Then Run Models." Urban Climate 24: 231–6.
- Wang, J., C. Wu, C. Zhang, W. Ju, X. Wang, Z. Chen, and B. Fang. 2018. "Improved Modeling of Gross Primary Productivity (GPP) by Better Representation of Plant Phenological Indicators from Remote Sensing Using a Process Model." *Ecological Indicators* 88: 332–40.
- Wang, H., D. Tetzlaff, J. Buttle, S. K. Carey, H. Laudon, J. P. McNamara, C. Spence, and C. Soulsby. 2019. "Climate-Phenology-Hydrology Interactions in Northern High Latitudes: Assessing the Value of Remote Sensing Data in Catchment Ecohydrological Studies." Science of the Total Environment 656: 19–28.
- Webb, E. K., G. I. Pearman, and R. Leuning. 1980. "Correction of the Flux Measurements for Density Effects due to Heat and Water Vapour Transfer." Quarterly Journal of the Royal Meteorological Society 106: 85–100.
- Whelan, A., R. Mitchell, C. Staudhammer, and G. Starr. 2013. "Cyclic Occurrence of Fire and Its Role in Carbon Dynamics along an Edaphic Moisture Gradient in Longleaf Pine Ecosystems." *PLoS One* 8(1): e54045.
- Wiesner, S., G. Starr, L. R. Boring, J. A. Cherry, P. C. Stoy, and C. L. Staudhammer. 2021. "Forest Structure and Composition Drive Differences in Metabolic Energy and Entropy Dynamics during Temperature Extremes in Longleaf Pine Savannas." Agricultural and Forest Meteorology 297: 108252.
- Wiesner, S., C. L. Staudhammer, C. L. Javaheri, J. K. Hiers, L. R. Boring, R. J. Mitchell, and G. Starr. 2019. "The Role of Understory Phenology and Productivity in the Carbon Dynamics of Longleaf Pine Savannas." *Ecosphere* 10(4): e02675.
- Wiesner, S., C. L. Staudhammer, H. W. Loescher, A. Baron-Lopez, L. R. Boring, R. J. Mitchell, and G. Starr. 2018. "Interactions among Abiotic Drivers, Disturbance and Gross Ecosystem

ECOSPHERE 17 of 17

Carbon Exchange on Soil Respiration from Subtropical Pine Savannas." *Ecosystems* 21(8): 1639–58.

- Wiesner, S., P. C. Stoy, C. L. Staudhammer, and G. Starr. 2020. "Using Metabolic Energy Density Metrics to Understand Differences in Ecosystem Function during Drought." *Journal of Geophysical Research – Biogeosciences* 125(3): e2019JG005335. https://doi.org/10.1029/2019JG005335.
- Wu, C., and J. M. Chen. 2013. "Deriving a New Phenological Indicator of Interannual Net Carbon Exchange in Contrasting Boreal Deciduous and Evergreen Forests." *Ecological Indicators* 24: 113–9.
- Wu, C., A. Gonsamo, C. M. Gough, J. M. Chen, and S. Xu. 2014. "Modeling Growing Season Phenology in North American Forests Using Seasonal Mean Vegetation Indices from MODIS." Remote Sensing of Environment 147: 79–88.
- Wu, C., D. Peng, K. Soudani, L. Siebicke, C. M. Gough, M. A. Arain, G. Bohrer, et al. 2017. "Land Surface Phenology Derived from Normalized Difference Vegetation Index (NDVI) at Global FLUXNET Sites." Agricultural and Forest Meteorology 233: 171–82.
- Yang, L., and A. Noormets. 2020. "Standardized Flux Seasonality Metrics: A Companion Dataset for FLUXNET Annual Product." Earth System Science Data Discussions 13: 1461–75. https://doi.org/10.5194/essd-2020-58
- Younes, N., K. E. Joyce, and S. W. Maier. 2021. "All Models of Satellite-Derived Phenology Are Wrong, but some Are Useful: A Case Study from Northern Australia." *International Journal of Applied Earth Observation and Geoinformation* 97: 102285.
- Younes, N., T. D. Northfield, K. E. Joyce, S. W. Maier, N. C. Duke, and L. Lymburner. 2020. "A Novel Approach to Modelling Mangrove Phenology from Satellite Images: A Case Study from Northern Australia." *Remote Sensing* 12(24): 4008.

- Yuste, J. C., I. A. Janssens, A. Carrara, L. Meiresonne, and R. Ceulemans. 2003. "Interactive Effects of Temperature and Precipitation on Soil Respiration in a Temperate Maritime Pine Forest." *Tree Physiology* 23(18): 1263–70.
- Zhang, W., G. Yu, Z. Chen, L. Zhang, Q. Wang, Y. Zhang, H. He, et al. 2020. "Attribute Parameter Characterized the Seasonal Variation of Gross Primary Productivity (αGPP): Spatiotemporal Variation and Influencing Factors." *Agricultural and Forest Meteorology* 280: 107774.
- Zhang, J., J. Xiao, X. Tong, J. Zhang, P. Meng, J. Li, P. Liu, and P. Yu. 2022. "NIRv and SIF Better Estimate Phenology than NDVI and EVI: Effects of Spring and Autumn Phenology on Ecosystem Production of Planted Forests." Agricultural and Forest Meteorology 315: 108819.
- Zhou, Y. K. 2018. "Comparative Study of Vegetation Phenology Extraction Methods Based on Digital Images." *Progress in Geography* 37(8): 1031–44.

SUPPORTING INFORMATION

Additional supporting information may be found in the online version of the article at the publisher's website.

How to cite this article: Gong, Yuan, Christina L. Staudhammer, Susanne Wiesner, Yinlong Zhang, Jeffery B. Cannon, and Gregory Starr. 2022. "Uncertainty in Parameterizing a Flux-Based Model of Vegetation Carbon Phenology Using Ecosystem Respiration." *Ecosphere* 13(5): e4101. https://doi.org/10.1002/ecs2.4101